IEEE Access
Multidisciplinary | Rapid Review | Open Access Journal

Received March 5, 2020, accepted March 25, 2020, date of publication April 8, 2020, date of current version April 27, 2020.

Digital Object Identifier 10.1109/ACCESS.2020.2986682

INVITED PAPER

Tunable Terahertz Graphene-Based Absorber Design Method Based on a Circuit Model Approach

MOHAMMAD BIABANIFARD[1], ARASH ARSANJANI[2], MOHAMMAD SADEGH ABRISHAMIAN[1], (Member, IEEE), AND DEREK ABBOTT[3], (Fellow, IEEE)

[1]Advanced Electromagnetic Laboratory, School of Electrical Engineering, K. N. Toosi University of Technology, Tehran 16315-1355, Iran
[2]Institute of Microwave and Photonic Engineering, Technische Universität Graz, 8010 Graz, Austria
[3]School of Electrical and Electronic Engineering, The University of Adelaide, Adelaide, SA 5005, Australia

Corresponding author: Mohammad Biabanifard (biabanifard.m@email.kntu.ac.ir)

ABSTRACT In this paper, a simple, fast, and novel method for designing a tunable terahertz absorber with arbitrary central frequency and desired fractional bandwidth is presented. The proposed absorber consists of a single layer periodic array of graphene ribbons (PAGRs), placed a quarter wavelength from a metallic ground, separated by a dielectric material. An analytical circuit model of the terahertz absorber is used to obtain analytical expressions for the input impedance of the proposed device. Then, a simple expression for determining the value of capacitance and the resonance conditions of the RLC circuit is used to achieve a terahertz absorber with arbitrary central frequency and desired fractional bandwidth. The proposed method is applicable for the design of both narrowband and broadband absorbers, with only one layer of graphene ribbons. Also, the presented method is applicable for designing ultra-wideband absorbers using multiple layered PAGRs. Full-wave numerical simulation is performed to verify the accuracy and validity of the presented method. Excellent performance of the proposed method in terms of computation time and memory resource and providing the desired terahertz absorber characteristics shows that our method is promising as a design approach for sensing, imaging and filtering applications.

INDEX TERMS Terahertz absorber, tunable bandwidth, circuit model, transmission line method, graphene.

I. INTRODUCTION

Terahertz technology, a significant step in the realization of high-speed devices, is not yet fully developed and the capabilities of terahertz waves are not fully realized. Therefore, the terahertz spectra (roughly from 0.1 to 10 THz), which is a bridge between microwave and infrared frequencies, is referred to as the terahertz gap. This region of the spectra is of significant interest for high-frequency applications [1]–[6]. Sensing, biosensing, imaging, indoor communications, and medical applications are among the applications that are currently being studied [1]–[6].

Nowadays, the use of metamaterials, which are artificial sub-wavelength composite materials, has facilitated the realization of terahertz devices for a number of applications. Moreover, because of the exceptional physical and electromagnetic properties of graphene, one layer of carbon atoms arranged in a honeycomb lattice [7], terahertz graphene-based absorbers have attracted considerable attention in the past decade [7].

Because of the capability of graphene in supporting Surface Plasmon Polaritons (SPPs) together with the tunability of graphene surface conductivity, surface plasmon polariton-based absorbers with tunable peak positions can be achieved [7]–[9]. There are a number of studies that have used different geometric structures to excite SPPs in a somewhat different manner. For instance, structures including graphene stacks [8], hybrid-patterned graphene metasurfaces [10], decussate graphene ribbon arrays [11], elliptical geometries [12], multi-layer graphene [13], [14], composite graphene-metal microstructures [15], periodically sinusoidally-patterned graphene [16], metasurface [17], graphene sheet and patterned graphene [18], [19] have been reported. However, all the methods presented in most of these studies usually require full-wave simulations for designing and analyzing the structure. In most cases, the structure is

The associate editor coordinating the review of this manuscript and approving it for publication was Jenny Mahoney.

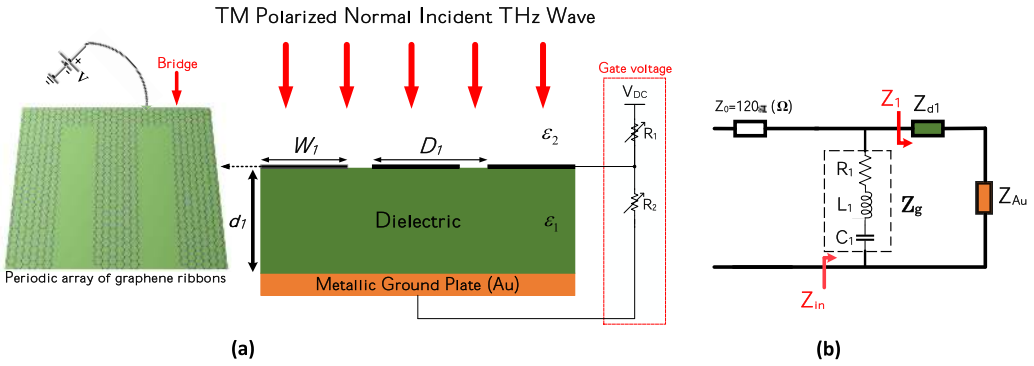

FIGURE 1. (a) The proposed terahertz absorber and (b) its circuit model.

complicated, and a full-wave simulation of these structures takes considerable time and resources to simulate. Also, the parametric study of the geometric properties of the structure is not discussed in most of these works. Furthermore, designing an absorber with arbitrary central frequency and desirable normalized bandwidth with 90% absorption is still challenging, and research in this area is ongoing. Andrea Alu and Nader Engheta are the pioneers who paved the way. They introduced modelling with lumped elements for devices at the terahertz and optical frequencies [20]–[23]. As a result of their studies, some authors have proposed analytical methods to design a terahertz absorber that are based on circuit models [13], [14], [24], [25]. Additionally, the description of graphene-based absorbers based on developed transmission line theory with explicit analytical expressions has been proposed and verified recently [13], [14], [19], [24], [25].

With all the work that has been carried out in pursuit of providing an efficient method for designing a terahertz absorber, still, there are some gaps in this field. Despite recent advances in circuit modeling, there is no clear and step by step procedure for the suitable design of terahertz absorbers with arbitrary central frequency and desired normalized bandwidth.

In this work, a simple, systematic, and efficient method for designing terahertz absorbers using recently developed circuit models [19], [24] is presented. The proposed method is general and can be applied to designing other types of active terahertz metamaterial devices. Compared to previous studies [14], [25]: (i) the method that is presented here can be used for designing both a tunable narrow- and wide-band terahertz absorption response through a simple and clear step by step procedure. These two different bandwidths for absorption response can be achieved by the same structure in which only one graphene-layer is used; (ii) the presented work has the advantage of realizing the desired central frequency (f_0) and the desired fractional bandwidth ($n = \frac{\mathrm{BW}}{f_0} \times 100$) of the structure with an analytical approach. The presented method can reduce design time. Moreover, by using more graphene layers and with the aid of optimization algorithms, such as genetic algorithms (GA) or a particle swarm optimization algorithm (PSO), the desired ultra-wideband absorber can be realized. The proposed structure can be fabricated through various methods [26], [27]. Lastly, the proposed method is used to design both a narrowband and an ultra-broadband absorber with a central frequency of 1 THz. A fractional bandwidth of 126% is obtained that is wider compared to 98% in a previously reported study [25]. Furthermore, the capability of our proposed method in designing both narrowband and broadband tunable absorbers at arbitrarily chosen frequencies of 3 and 4 THz is investigated, as a case study.

II. STRUCTURE AND CIRCUIT MODEL

A schematic of the unit cell of our absorber showing the incident terahertz wave radiation is given in Fig. 1. The absorber structure consists of one layer of PAGRs (Periodic Array of Graphene Ribbons), a dielectric substrate with the thickness of a quarter wavelength and a gold metal ground layer. Note that, D_1 and W_1 are the period and the width of the PAGRs, respectively. The structure is illuminated through a Transverse Magnetic (TM) polarized wave at normal incidence, which is the most practical case. A conductivity of $\sigma = 4 \times 10^7$ S/m is assumed for the Au reflector [25]. Also, the Au reflector is considered to be sufficiently thick to block the incident terahertz wave, which is typically selected based on the previous studies to be 1 μm. Another important issue that needs to be considered is the selection of the appropriate dielectric material, which has a direct impact on the fabrication process and the lifetime of the device. The polyethylene Cyclic Olefin Copolymer (TOPAS COC with $n_p = 1.53$) is a clear, stiff amorphous thermoplastic copolymer that delivers fluoropolymer-like electrical properties for advanced electronic applications. This substance can be readily injection molded, or extruded into sheets that facilitates manufacture and moreover, it is resistant to most acids and solvents. This polymer has a near zero hygroscopicity [28] and very low absorption that makes it an appropriate material for terahertz absorption applications [29], [30]. The Fermi level of the graphene layer can be tuned by varying the gate voltage [31], [32], which can be provided by an external bias circuit, as shown in Fig. 1. So, instead of re-optimizing and re-fabricating the device, the absorption spectra can be dynamically tuned by a small change in the

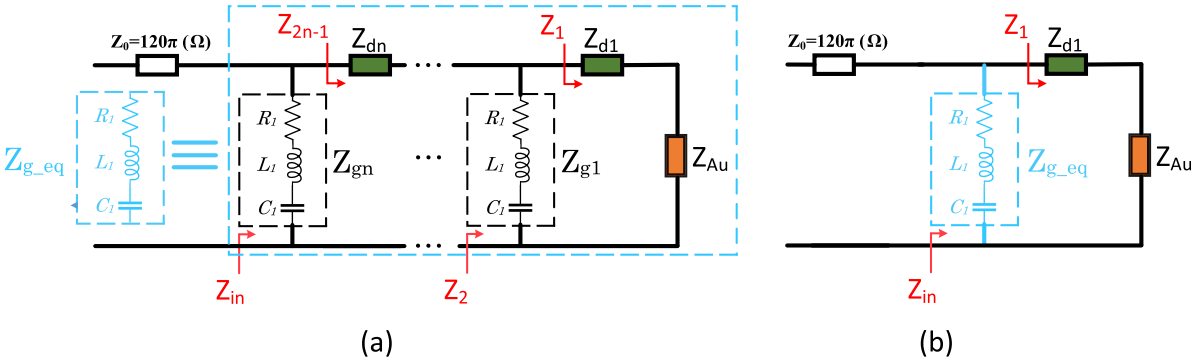

FIGURE 2. (a) Circuit model of the absorber with graphene n-layer structure and (b) the equivalent circuit of the absorber with *n* graphene layers (PAGRs).

Fermi energy of the graphene layer. Using transmission line theory together with an analytical circuit model for graphene ribbons, the equivalent circuit model of the studied structure is presented as shown in Fig. 1(b) [19], [24], [33]. In pursuit of presenting a description of the circuit model; the gold layer at the bottom of the structure can be considered as a short circuit to a good approximation [19], [25], [33]. The dielectric layer can be modeled as an ideal transmission line, as by adjusting its thickness it represents capacitive1 or inductive element behavior [34], and since the thickness of the graphene layer compared to typical terahertz wavelengths is ultra-thin, its thickness can be ignored, and the graphene layer can be considered as a point load Z_g [18], [24], see Fig. 1. It is demonstrated that the impedance of the periodic arrays of graphene ribbons is composed of an infinite number of parallel RLC circuits, each representing a resonating mode of the graphene ribbon [33]. These modes are Fabry-Pérot resonances of a graphene plasmon trapped within the finite width of a graphene ribbons [33].

By designing the proposed structure near its first resonance frequency, the effect of the higher-modes can be ignored [13], [25], [33]. In this work, the thickness of the graphene layer is considered to be $\Delta = 1$ nm (three monolayers). In a number of references this thickness is considered for graphene [19], [25] and realized [26]. By considering $\exp(j\omega t)$ as the time-harmonic dependency, numerical modeling of the graphene layer with permittivity of $\varepsilon_{GR} = \varepsilon_0 - j\sigma_{GR}/(\Delta\omega)$ is carried out, where σ_{GR} is the graphene surface conductivity and can be easily derived using the well-known Kubo formula [35]. Intraband and interband electron transitions are two main components of the graphene surface conductivity. At sufficiently low frequencies when the relation $\hbar\omega \ll 2\mu_c$ is satisfied, the intraband transitions are considered to be the sole source of the surface conductivity of the graphene, which can be written as [36], [37]:

$$\sigma_{GR}(\omega, \mu_C, \tau, T) = -j\frac{e^2 k_B T}{\pi\hbar^2(\omega - j\tau^{-1})} \times \left[\frac{\mu_c}{k_B T} + 2\ln\left[\exp\left(-\frac{\mu_c}{k_B T}\right)\right] + 1\right] \quad (1)$$

where $-e$ is the electron charge, T is the temperature, k_B is the Boltzmann constant, $\hbar$ is the reduced Planck constant, μ_c is the chemical potential of the graphene, and τ is the relaxation time of electrons. In this work, the ambient temperature ($T = 300$ K) is used.

The circuit model can be used to realize the desired absorption spectra for the proposed absorber. Since in the terahertz gap, the gold reflector works as an acceptable metallic surface [19], [25], the incident terahertz wave cannot transmit through this layer. As a result, the terahertz wave either reflects from its surface, or it can be absorbed completely by it. Therefore, for a desired reflection, the absorption (A) can be calculated by $A = 1 - |\Gamma_{in}|^2$; where $\Gamma_{in} = \frac{Z_{in}-Z_0}{Z_{in}+Z_0}$. Based on the electromagnetic wave theory [34], Z_1 with the normal incident TM polarized terahertz wave can be derived as $Z_1 = Z_d\frac{Z_{Au}+jZ_d\tan(\beta_d l)}{Z_d+Z_{Au}j\tan(\beta_d l)}$, where $Z_d = Z_0/n_p$, β_d, and l respectively represent the impedance of the dielectric middle layer, the propagation constant of the propagating terahertz wave in the dielectric substrate, and the length of the transmission line which is presented as d_1 as seen in Fig. 1. The input impedance of the absorber can be calculated by $Z_{in} = Z_g \parallel Z_1$. The conductance of the gold layer is high enough to be considered as a short circuit in the terahertz region ($Z_{Au} = 0$) [19], [25] which leads to $Z_1 = jZ_d\tan(\beta_d l)$. Besides, Z_g is defined as follows [13], [19], [24], [25]:

$$Z_g = R_1 + j\omega L_1 + \frac{1}{j\omega C_1}. \quad (2)$$

The values of R_1, L_1, and C_1 is calculated as follows [33]:

$$R_1 = \frac{\hbar^2}{e^2 E_f \tau}\frac{K_1 P^2}{\pi S_1^2}\ L_1 = \frac{\hbar^2}{e^2 E_f}\frac{K_1 P^2}{\pi S_1^2}\ C_1 = \frac{\varepsilon_{eff}}{q_{11}}\frac{\pi S_1^2}{K_1 P^2} \quad (3)$$

where S_1 is the integral of the eigenfunctions of the equation governing the surface current given in Table 1 of Khavasi and Rejaei [33] and $Q_1 = q_1(\pi/W)$ is the eigenvalue of the same equation while $\varepsilon_{eff} = \varepsilon_0(\varepsilon_1 + \varepsilon_2)/2$ is the average permittivity of the dielectric materials that surrounds the graphene on both sides as seen in Fig. 1.

III. DESIGN PROCEDURE

This article presents three simple but powerful methods for designing an absorber with arbitrary central frequency and

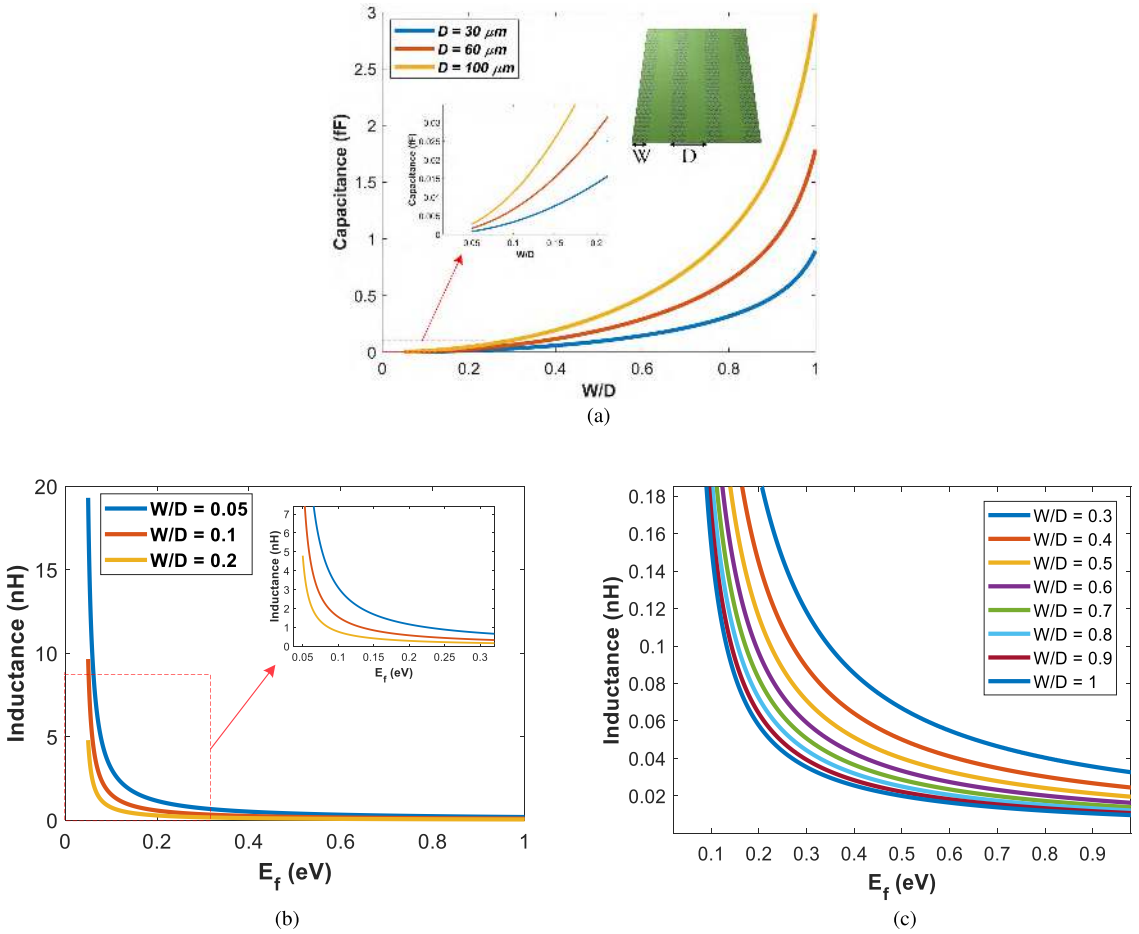

FIGURE 3. (a) Capacitance of the PAGRs (C_1) as a function of W/D ratio (b) inductance of the PAGRs (L_1) as a function of graphene Fermi energy with $D = 100$ μm (c) inductance of the PAGRs (L_1) as a function of graphene Fermi energy with $D = 100$ μm.

desired normalized bandwidth in the terahertz regime. With only one graphene-layer, both narrowband and broadband absorbers can be efficiently designed using the presented method. Also, by using more layers of graphene ribbons, our method is applicable to design an ultra-wideband absorption response.

A. METHOD OF DESIGN

In this part, we show procedure for designing the aforementioned absorption responses using circuit principles. To do this, as the first step, the dielectric thickness (d_1) should be selected as a quarter wavelength. Then the amount of normalized bandwidth, $\Delta f/f_0$, where f_0 is the central frequency, must be selected as desired. Continuing the design, the equivalent capacitance (C_1) must be calculated. It is important to note that the amount of equivalent capacitance of the PAGRs is directly related to the absorption bandwidth of the structure. The lesser capacitance we have, the narrower bandwidth we could gain. On the other hand, the larger capacitance we have, the broader bandwidth we could have; thus, we must calculate the required amount of capacitance to satisfy the desired fractional bandwidth (n). Given Eqn. 3, the amount of capacitance is only dependent on the geometrical structure of the device and the material surrounding it (ε_{eff}). In our case, the material underneath the PAGRs is TOPAS ($\varepsilon_1 = 2.34$, see Fig. 1(a)) and the upper material is air ($\varepsilon_2 = 1$). Thus, if due to geometrical limitations, the required amount of capacitance cannot be satisfied, changing the dielectric material beneath the PAGRs can be assist to meet the goal. The detail of this procedure with analytic mathematical calculations is brought in the next sections.

Now, by having C_1, we calculate the required amount of inductance (L_1) to have the resonance in the desired central frequency. Then, using a graphical solution with the aid of Fig. 3, we determine the amount of graphene chemical potential. Finally, utilizing Fig. 4, we determine the required amount of τ to have R_1 equal to free space impedance or as close as possible.

This method takes advantage of excellent performance in terms of computational time and memory resources. For the studied structures, it takes more than 10 min to complete analysis using the frequency domain electromagnetic solver with a computer possessing the following characteristics: processor, Intel(R) Core(TM) i7-7700 CPU @ 3.60 GHz:

installed memory (RAM), 32.0 GB. While for the same computer by exploiting this method, it takes only less than 0.5 s to complete the analysis and get the results.

B. SINGLE-LAYER NARROWBAND ABSORBER DESIGN METHOD

Let us first design an absorber with a central frequency of f_0. As there is no transmission through the absorber due to the gold (Au) reflective layer, perfect absorption at the central frequency can be achieved by setting $\Gamma_{in} = 0$, which means $Z_{in} = Z_0$. Perfect absorption can be derived merely by considering $\beta_d l = 90^o$ where it can be achieved by choosing the thickness of the dielectric material by the equation $l = c/4n_p f_0$, where c is the velocity of light. It consequently results in $Z_1 = \infty$ and $Z_{in} = Z_g$ as seen in Fig. 1. As a result, the Z_1 impedance acts as an open circuit.

Therefore, perfect absorption criteria can be achieved by satisfying $Z_g = Z_0$. It implies that $R_1 = Z_0 = 120\pi\ \Omega$ and $\mathrm{Im}\left(Z_g\right) = j\omega_0 L_1 + \frac{1}{j\omega_0 C_1} = 0$, which leads to the equation $L_1 = \frac{1}{C_1\omega_0^2}$. However, these criteria only provide perfect absorption at the central frequency and are not sufficient enough for designing an absorber with desired bandwidth. By selecting $A > 0.9$ as an acceptable absorption criterion in the desired spectral range, extra measures are required to meet this absorption goal. By choosing an appropriate n, which is the fractional bandwidth of the absorption spectra ($N = \frac{\Delta f}{f_0}$, $n = N \times 100$), the equation ($|\Gamma_{in}| < 0.3162$) must be satisfied in order to realize the $A > 0.9$ criteria [24]. Let us consider an absorption of more than 90% in the interval of $\left[f_0 - \Delta f/2, f_0 + \Delta f/2\right]$.

To achieve the desired upper and lower frequency of the absorption, Γ_{in} must be calculated in the interval frequencies; hence, Z_1 and Z_{in} must be calculated again at the upper and lower frequencies of the absorption spectra:

$$Z_1 = jZ_d \tan\left(\beta_d l\right) = jZ_d \tan\left(\frac{\pi}{2}\frac{f}{f_c}\right) \tag{4}$$

$$Z_g = R_1 + j\omega L_1 + \frac{1}{j\omega C_1} = R_1 + j\left(\frac{\omega^2 L_1 C_1 - 1}{C_1\omega}\right)$$
$$\Rightarrow Z_g = R_1 + j\left(\frac{\frac{\omega^2}{\omega_0^2} - 1}{C_1\omega}\right), \quad \text{where } L_1 = \frac{1}{C_1\omega_0^2}. \tag{5}$$

If a narrowband absorption response is needed ($n \leq 10\%$), by assuming that $Z_{1\,@f=f_0\pm\Delta f/2} \approx \infty$, Z_1 can still be treated as an open circuit. Continuing with this consideration, the mismatch in the absorber occurs because of the imaginary part of Z_{in} and not because of the real part. As seen in (5), the only value that changes with frequency is the imaginary part which means that this term is frequency dependent. By considering $Z_{in} = R + jX$ and $Z_0 = R_0$, it can be concluded that:

$$|\Gamma_{in}| = \left|\frac{X}{\sqrt{4R_0^2 + X^2}}\right| \rightarrow |X|^2 = \frac{4|\Gamma_{in}|^2 R_0^2}{1 - |\Gamma_{in}|^2}. \tag{6}$$

By considering $|\Gamma_{in}| < 0.3162$ to have the perfect absorption ($A > 0.9$), and the assumption of $R = 120\pi\ \Omega$, solving (6) results in $|X| \leq 80\pi$. As a result, the equivalent capacitance of the Z_g for the desired fractional bandwidth (n) and the central frequency of f_0 can be calculated as below:

$$|X|_{@f=f_0+f/2} = \left|\frac{\left(1+\frac{N}{2}\right)^2 - 1}{\left(C_1\left(1+\frac{N}{2}\right)\omega_0\right)}\right| \rightarrow C_1 = \frac{\left(1+\frac{N}{2}\right)^2 - 1}{|X|\left(1+\frac{N}{2}\right)\omega_0}. \tag{7}$$

C. SINGLE-LAYER WIDEBAND ABSORBER DESIGN METHOD

Designing a wideband absorption response is a different task since in the design procedure, Z_1 is no longer infinite. Here, Z_1 is not infinite because it is not possible to approximate $f_0 \approx f_0 \pm \Delta f/2$ and as a result, the relation $Z_{in} \approx Z_g$ which is achieved for narrowband absorption is not valid for achieving a broadband response. Therefore, a different approach to design the desired absorber is required. First, the dielectric thickness will be set equal to $l = c/4n_p f_0$. Given that Z_1 is not infinite at $f_0 \pm \Delta f/2$, the calculation of the input impedance will be different. By considering $\omega = (1 + N/2)\,\omega_0$, Z_{in} is calculated as presented below:

$$Z_{1\,@f_0+\Delta f/2} = jX_2 = jZ_d \tan\left(\frac{\pi}{2}\left(1 + \frac{N}{2}\right)\right) \tag{8}$$

that results in:

$$Z_{in} = Z_1 \parallel Z_{g_1} = jX_2 \parallel (R_1 + jX_1)$$
$$\mathrm{Re}\left(Z_{in}\right) = R_{eq} = \frac{R_1 X_2^2}{R_1^2 + (X_1 + X_2)^2}$$
$$\mathrm{Im}\left(Z_{in}\right) = X_{eq} = \frac{\left(R_1^2 + X_1^2\right)X_2 + X_1 X_2^2}{R_1^2 + (X_1 + X_2)^2} \tag{9}$$
$$|\Gamma_{in}|^2 = 1 - \frac{4R_0 R_{eq}}{\left(R_{eq} + R_0\right)^2 + X_{eq}^2} \leq 0.1 \tag{10}$$

that can be substituted to extract a more explicit equation as below:

$$\frac{480\pi R_1 X_2^2\left[R_1^2 + (X_1 + X_2)^2\right]}{U}$$
$$\geq 0.9\,U = \left[R_1 X_2^2 + 120\pi\left(R_1^2 + (X_1 + X_2)^2\right)\right]^2$$
$$+\left[\left(R_1^2 + X_1^2\right)X_2 + X_1 X_2^2\right]^2. \tag{11}$$

Thus, having X_2 from Eqn. 8, and by the aid of optimization algorithms such as the genetic algorithm (GA) which reflects the process of natural selection where the fittest individuals are selected for reproduction in order to produce offspring of the next generation, the best values for X_1 and R_1 can be calculated. In this work, we have used the GA which is reported in [14]. Then, C_1 can be calculated using 7.

D. ULTRA-WIDEBAND DESIGN APPROACH

In the circuit model point of view, Z_{in} is frequency dependent. As a result, achieving Im $(Z_{in}) = 0$ and Re $(Z_{in}) = Z_0$, simultaneously, over a wide range of frequencies which can lead to an ultra-wideband absorption is not a simple task. Thus, for achieving these goals, adding more graphene layers can lead to improved controllability of the input impedance by changing the Fermi energy of each graphene layer independently. The multi-layer structure can also add more complexity to the circuit model of graphene. Fortunately, this issue was resolved with the emergence of optimization algorithms such as GA, particle swarm optimization (PSO) which is a computational method that optimizes a problem by iteratively trying to improve a candidate solution with regard to a given measure of quality. To simplify the design procedure and its description we consider the circuit model of the graphene n-layer structure as an equivalent single-layer graphene absorber, as shown in Fig. 2(a) and 2(b). By this assumption, from the circuit point of view, the absorber with n-layer of PAGRs can be modeled as an equivalent circuit of RLC. As a result, the ultimate goal, which is designing an ultra-wideband absorber, can be achieved. The proposed solution can be presented from another point of view: in the studied structure, each graphene layer (PAGRs) combined with the dielectric and the metallic reflecting surface can be considered as an asymmetric Fabry-Pérot resonator, the graphene layer plays a role of partially reflecting mirror and the Au reflecting layer plays a role of fully reflecting mirror. Thus, each graphene layer absorbs a specific range of frequencies, and by adding more layers of graphene to the structure, an absorption over 90% can be extended up in a wide range of frequencies leading to an ultra-wideband absorption.

GRAPHENE-BASED ABSORBER REALIZATION

The purpose of this section is to obtain the numerical values of four parameters: D, W, μ_c, and τ that can be implemented in practical cases. The realization of the absorber depends on the validity of the geometry and material characteristics of the graphene. After calculating the values of R_1, L_1 and C_1 from the previous section, the geometry and characteristics of the graphene absorber must be realized. It is important to know that there are always limitations in the selection of these parameter values. These values are selected in such a way that they can be implemented in practical cases. The limitations are: (i) the fill factor of the graphene array (W/D) must be smaller than unity; (ii) the structure must be a sub-wavelength one to guarantee the validity of the circuit model [33], and (iii) the relaxation time and the Fermi energy of the graphene must be considered larger than $\tau = 0.01$ ps and in the range of $\mu_c = 0$ to 1 eV, respectively [38]–[43]. In practice, the relaxation time (τ) can be tuned by the Fermi energy E_F, which is a fundamental parameter of the conductivity model. The equation $\tau = \mu E_F / e v_F^2$ indicates the dependency of the relaxation time to the graphene Fermi energy and electron mobility, where μ is the electron mobility and $v_F = 10^6$ m/s is the graphene Fermi velocity [25]. It should be noted that the electron mobility of graphene on a substrate, varies from about 0.1 m^2/Vs [31] to 6 m^2/Vs [44], depending on the quality of the fabrication process. Also, this parameter is highly influenced by the substrate material [44]–[46]. In the following, by exploiting graphical solutions, it is shown how the values of inductor, capacitor, and resistor fall within the desired range for an absorber in the terahertz regime.

The period, D, of graphene ribbons is arbitrarily selected. To this day, conventional structures with desirable performance in the terahertz band typically have the range $D = 2$ μm to 120 μm [18], [19], [25], [47]. The amount selected will affect the capacitance value that has a direct impact on determining the amount of absorption bandwidth.

Fig. 3(a) illustrates the equivalent capacitance of the PAGRs as a function of fill factor (W/D) for $D = 30$, 60, and 100 μm. The increase in the fill factor value increases the equivalent capacitance C_1 which is desirable for designing broadband absorbers. Also, reducing W/D, reduces the capacitance to the atto-farad (10^{-18}) range, which is very suitable for the realization of ultra-narrowband absorbers. Therefore, for broadband absorbers, selecting W/D values toward one is desirable, and for the narrowband case, it is appropriate to select W/D values toward zero. As a result, in a graphical point of view, the ratio of the width to the period of the ribbons (W/D) can be determined from Fig. 3(a). Then, the graphene chemical potential is determined from the inductance diagram, which for different values of the fill factor is plotted in Fig. 3(b) and Fig. 3(c). As seen, different values in the nano-Henry range are achieved by the use of chemical potential tunability. Finally, the relaxation time of electrons (τ) must be determined by matching the resistance of R_1 to the Z_0. Figs. 4(a), 4(b), 4(c), and 4(d) reported on the amount of R_1 with different values of the width over the period of PAGRs ($W/D = 0.05, 0.1, 0.5$, and 0.9 respectively) and chemical potential as a function of relaxation time. These figures indicate that the value of R_1 can fall around the Z_0 with the most practical interval of the relaxation time $(\tau = 0.1 - 1$ ps). So, using reliable and practical graphene parameters, the realization of a terahertz graphene absorber by exploiting these figures for designing purpose can be readily achieved. Using (3), Q_1 can be written as:

$$Q_1 = \frac{1}{C_1} \frac{2\varepsilon_{\text{eff}} S_1^2}{D}, \tag{12}$$

which by having the amount of Q_1, according to the Table. 1 the ratio of W/D is calculated. Then, the chemical potential of the graphene is determined according to (3), and can be written as:

$$E_F = \frac{1}{L_1} \frac{D\pi\hbar^2}{e^2 S_1^2}. \tag{13}$$

Finally, according to the same equation, the relaxation time of graphene electrons and the electron mobility of the graphene

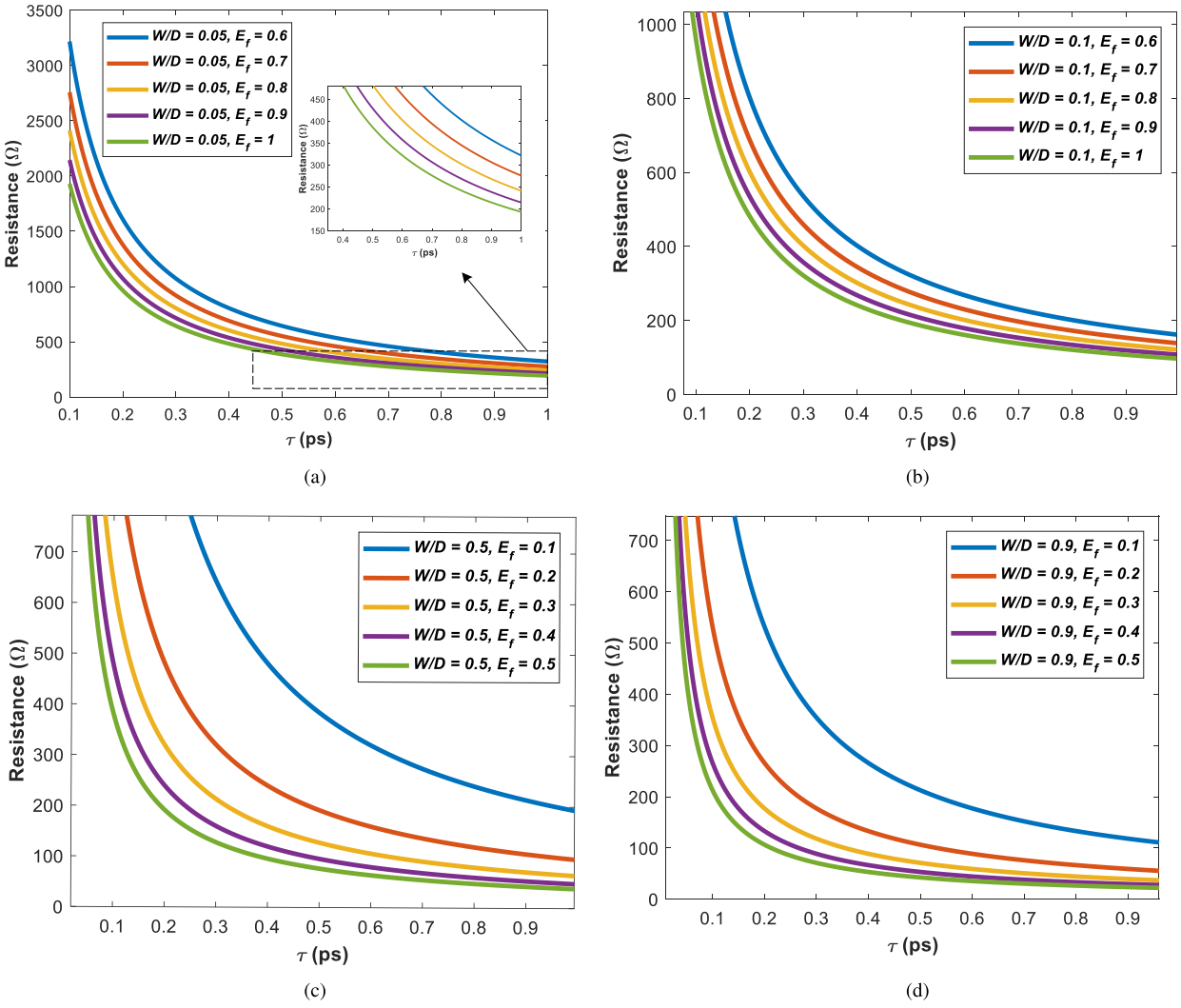

FIGURE 4. (a) Resistance of the PAGRs (R_1) as a function of graphene relaxation time with $D = 100$ μm (b) Resistance of the PAGRs (R_1) as a function of graphene relaxation time with $D = 100$ μm (c) Resistance of the PAGRs (R_1) as a function of graphene relaxation time with $D = 100$ μm (d) Resistance of the PAGRs (R_1) as a function of graphene relaxation time with $D = 100$ μm.

TABLE 1. Eigenvalues of the equation governing the surface current on graphene ribbons [24], [33]. W/D is the graphene fill factor and q_1 is the first eigenvalue of the PAGRS.

W/D	0.05	0.1	0.2	0.3	0.4	0.5	0.6	0.7	0.8	0.9	1
$q_1 W/\pi$	0.742	0.734	0.725	0.710	0.689	0.658	0.620	0.571	0.507	0.420	0.28

is determined by:

$$\tau = \frac{L_1}{R_1} = \frac{\mu E_F}{e v_F^2} \rightarrow \mu = \frac{L_1 e v_F^2}{R_1 E_F}. \tag{14}$$

This indicates the realization of the absorber is depended on the ratio of L_1/R_1 and is required to satisfy the practical value of the graphene electron mobility (0.1 m^2/Vs $< \mu <$ 6 m^2/Vs). Exploiting these equations besides applying the graphene parameters limitations, the lower and upper bounds for the C_1 and L_1 values with the determined D can be achieved: with an appropriate approximation $S_1^2 \cong (8/9)\, W$ can be considered [25]. So, the amount of S_1^2/D can be considered equal to $\frac{8}{9}\frac{W}{D}$. Thus, using (3), the upper and lower bounds of the C_1 and L_1 can be achieved.

IV. RESULTS AND DISCUSSION

Five graphene-based terahertz absorbers with only one layer of PAGRs and one ultra-wideband absorber with two graphene-layer is designed as numerical examples to validate the proposed method; where the designed parameters are given in Table 2 and Table 3, respectively. In order to investigate the performance of the presented method in designing the narrow and ultra-wideband absorption, two absorbers with the central frequency of 1 THz is designed

TABLE 2. Designed parameters of the absorbers with only one graphene-layer.

	D(μm)	W(μm)	$d_1(\mu$m)	μ_c(eV)	τ (ps)	f_0 (THz)	f_0/BW%
Absorber 1	29.5	8	49	0.036	2.675	1	4.6
Absorber 2	29.5	4.66	16.33	0.2	0.89	3	4.67
Absorber 3	29.5	12.5	16.33	0.52	0.115	3	43
Absorber 4	29.5	4.51	12.25	0.34	0.0536	4	5.8
Absorber 5	29.5	10	12.25	0.8	0.1	4	37

TABLE 3. Designed parameters of the ultra-wideband Absorber with two graphene-layer.

	Layer 1	Layer 2	f_0 (THz)	f_0/BW%
The proposed ultra-thin	(PAGRs)	(PAGDs)		
	$\mu_{c_1} = 0.695$ eV	$\mu_{c_2} = 0.001$ eV	1	126.4
	$D_1 = 80\ \mu$m	$D_2 = 40\ \mu$m		
wideband absorber	$W_1 = 73.22\ \mu$m	$W_2 = 38.12\ \mu$m		
	$d_1 = 49\ \mu$m	$d_2 = 49\ \mu$m		

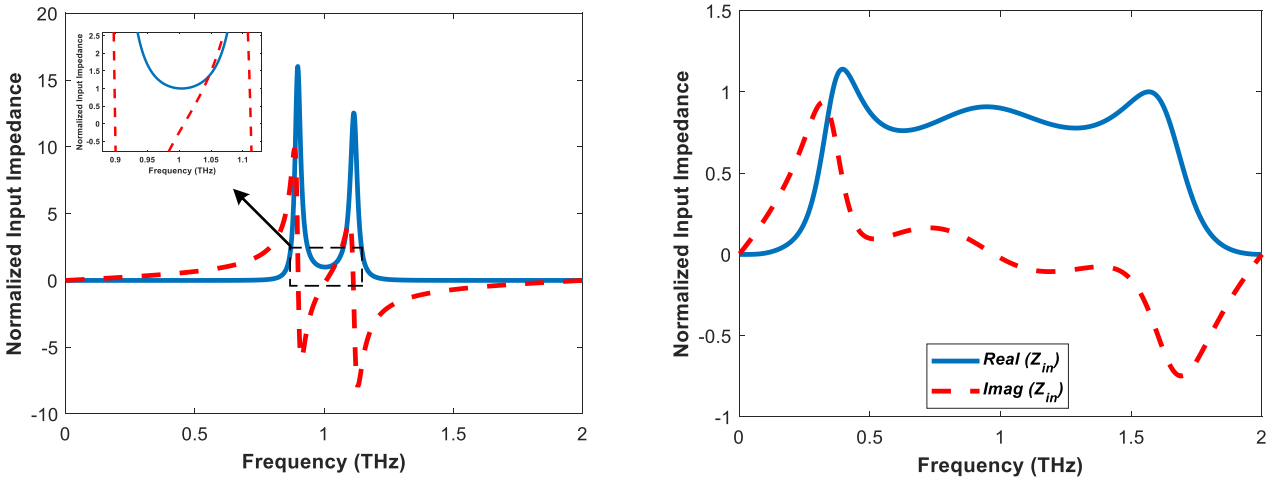

(a) (b)

FIGURE 5. (a) The normalized input impedance of the narrowband absorber 1 in Table. 2 (b) The normalized input impedance of the ultra-broadband absorber (the absorber in Table 3).

which the fractional bandwidth of these structures are plotted in Fig. 5(a) and 5(b), respectively. Also, the absorption spectra of these structures are plotted in Fig. 6(a) and Fig. 6(b), respectively. The fractional bandwidths of these structures are 4.6% and 126%, respectively. The perspective of the ultra-wideband absorber is depicted in Fig. 6(c). The near-unity absorption obtained by these structures; shows their potential in sensing and imaging applications. The absorption spectra is obtained by the full-wave numerical modeling (dash lines), the Finite Element Method (FEM) while the frequency-domain solver is exploited [51]–[53]. On the other hand, an easy to implement MATLAB code which represents the circuit model approach (solid lines) is performed.

The results obtained by the circuit model and the FEM method exhibits similar characteristic; thus, showing the validity of the proposed method. Fig. 6(d) is reported to show the tunability of the designed absorber with the central frequency of 3 THz. As depicted in this figure, the peak's position is sensitive to the Fermi energy of the graphene and can be shifted as desired. The E-field distribution of absorber 1 in Table. 2 at its resonance frequency is plotted in Fig. 7. As seen, the excitation of SPPs are much more at the ribbon edges. Moreover, full distribution of the E-field and H-field from different perspective are provided in supplementary data of this work. One of the most significant advantages of the proposed method is that it can design a reliable absorber with arbitrary central frequency and the desired fractional bandwidth. This claim is verified through several numerical examples. Figs. 8(a) and 8(b) show how the proposed method is capable of being applied for designing both narrow-band and broad-band absorbers at the same frequency. The central frequency of these absorbers is chosen arbitrarily, at 3 and 4 THz. These absorption spectra are highly valuable in sensing and filtering applications point of view.

Concerning the possible fabrication errors, the performance of the studied configuration with $\pm 5\%$ ribbon width variations for the designed wideband absorber at $f_0 = 4$ THz

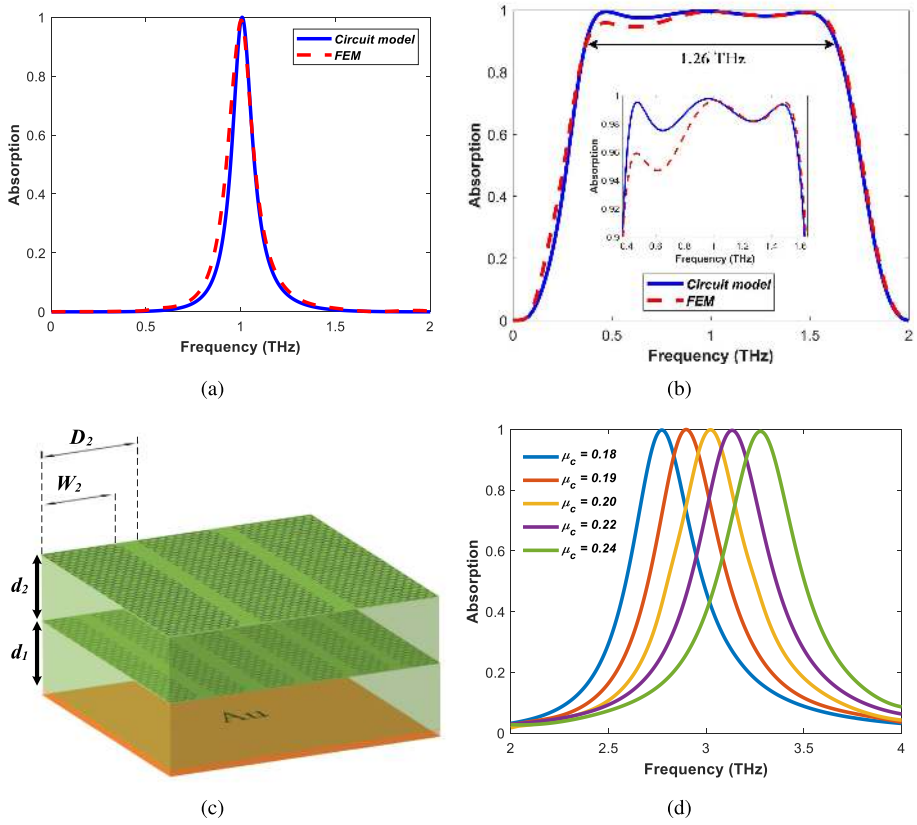

FIGURE 6. (a) Absorption spectra of the narrow band absorber with central frequency of $f_0 = 1$ THz (Absorber 1 in Table 2) (b) ultra-wideband absorption spectra of the designed absorber with central frequency of $f_0 = 1$ THz (the absorber in Table. 3), (c) configuration of ultra-wideband absorber with two PAGRs (The absorber in Table. 3), and (d) absorption spectra of absorber 2 in Table 2 with tunability of the peak's frequency, calculated by FEM.

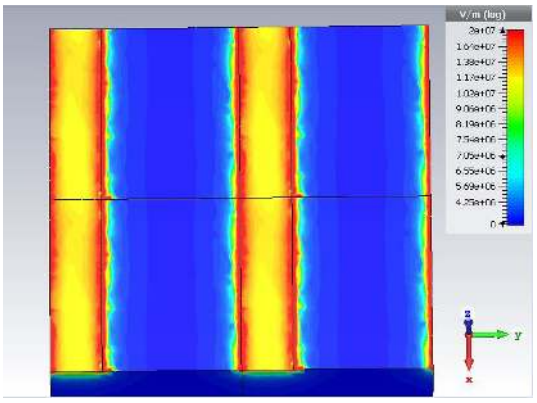

FIGURE 7. E-field distribution of Absorber 1 in Table 2 at its resonance frequency.

is illustrated in Fig. 8(c). As seen, with increasing the ribbon width, the central frequency of absorption spectra shifts a bit towards the lower frequencies, but the performance of the device does not change significantly. It is worth discussing the efficiency of our proposed method compared to the commonly used methods in the literature. Regarding provision of an efficient, simple, and fast graphical solution for designing the desired terahertz absorber, the proposed method reduces the design costs compared to the situations with the use of full-wave numerical modeling for tuning and designing the absorber.

Considering the fabrication challenges and for simplicity, we entirely presented our approach for the single-layer graphene absorber and obtained both narrow and broadband responses. However, a narrower or broader response can be achieved using more layers of graphene ribbons. The proposed method can be developed for this scenario. Moreover, the studied structure absorbs only TM polarized terahertz waves where if a polarization-insensitive absorber is to be a case, using 2D arrays of graphene Disks instead of ribbons may meet the goal. The description of the structure as circuit elements besides the ease of fabrication and exploiting Chemical Vapor Deposition (CVD) or other fabrication methods, which are thoroughly described in [26], [27], nominate the proposed method to be practically used in designing terahertz active metamaterial devices.

Finally, a fair comparison of the presented method with previous works on designing an ultra-wideband or broadband absorber is given in Table. 4. It should be noted that our proposed method, improves the normalized bandwidth of the previous works, in addition to the advantage of tunability

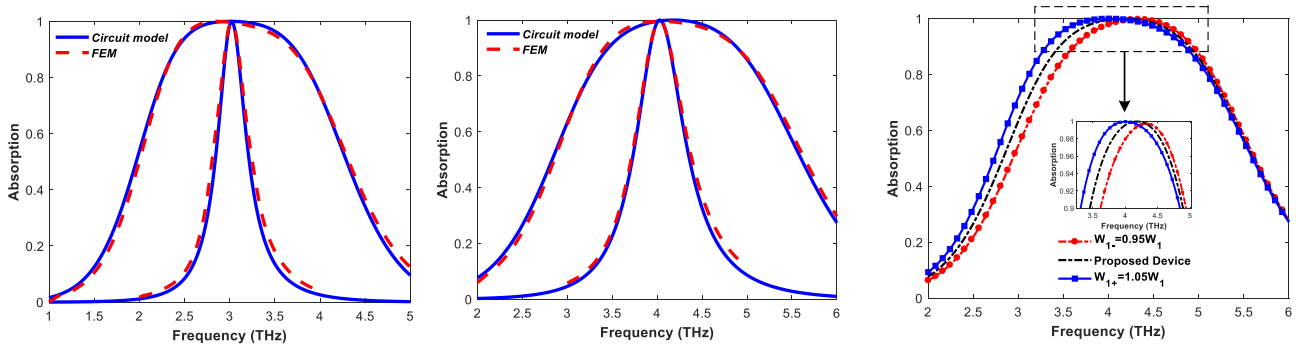

FIGURE 8. (a) Absorption spectra of Absorber 2 (narrowband) and Absorber 3 (broadband) in Table. 2 (b) absorption spectra of Absorber 4 (narrowband) and Absorber 5 (broadband) in Table. 2 (c) Absorption spectra of the structure for different ribbon widths, calculated by FEM.

TABLE 4. Comparison of the proposed ultra-wideband device with previous works.

	Metal layer	Thickness (μm)	f_0(THz)	BW/f_0%
[48]	1	1.8	4.96	7.9
[49]	1	3.4	4.79	17.1
[50]	5	9	1.96	28
[8]	5	4.5	3.07	31.9
[25]	1	25	2	88
[25]	1	50	1	98
This Work	2	98	1	126.4

of the peak's position, easy circuit analysis, designing an absorber with desired normalized bandwidth, and decreases the cost of designing in terms of computation time and memory sources.

V. CONCLUSION

By exploiting one graphene/dielectric layer placed on a metallic plate an efficient and novel method to design a terahertz absorber is proposed and investigated. The proposed method is applicable for designing both narrowband and broadband absorbers with analytically determined central frequency and the normalized bandwidth. A metallic ground at the bottom of the structure is used to restrict the transmission. The incident electromagnetic wave is trapped efficiently resulting in strong excitation of graphene surface plasmons. The design takes advantage of circuit theory and the graphene surface conductivity tunability that leads to a change in the peak's position of the absorption. The obtained results with the proposed method are verified through full-wave numerical modeling simulations. Ease of fabrication and also lower design costs regarding runtime and memory sources nominates the proposed method and configuration to have the potential to be utilized in designing and also the fabrication of tunable sensors, filters, and terahertz imaging systems.

REFERENCES

[1] C. M. Watts, X. Liu, and W. J. Padilla, "Metamaterial electromagnetic wave absorbers," *Adv. Mater.*, vol. 24, no. 23, pp. OP98–OP120, Jun. 2012.
[2] Y. Chen, H. Liu, M. J. Fitch, R. Osiander, J. B. Spicer, M. Shur, and X.-C. Zhang, "THz diffuse reflectance spectra of selected explosives and related compounds," *Proc. SPIE*, vol. 5790, pp. 19–25, May 2005.
[3] C. Yu, S. Fan, Y. Sun, and E. Pickwell-MacPherson, "The potential of terahertz imaging for cancer diagnosis: A review of investigations to date," *Quant. Imag. Med. Surg.*, vol. 2, no. 1, pp. 33–45, Mar. 2012.
[4] S. Fan, Y. He, B. S. Ung, and E. Pickwell-MacPherson, "The growth of biomedical terahertz research," *J. Phys. D, Appl. Phys.*, vol. 47, no. 37, Sep. 2014, Art. no. 374009.
[5] L. Ye, K. Sui, Y. Liu, M. Zhang, and Q. H. Liu, "Graphene-based hybrid plasmonic waveguide for highly efficient broadband mid-infrared propagation and modulation," *Opt. Express*, vol. 26, no. 12, p. 15935, Jun. 2018.
[6] H.-T. Chen, W. J. Padilla, J. M. O. Zide, A. C. Gossard, A. J. Taylor, and R. D. Averitt, "Active terahertz metamaterial devices," *Nature*, vol. 444, no. 7119, pp. 597–600, Nov. 2006.
[7] A. K. Geim and K. S. Novoselov, "The rise of graphene," in *Nanoscience and Technology: A Collection of Reviews from Nature Journals*. Singapore: World Scientific, 2010, pp. 11–19.
[8] Y. Dong, P. Liu, D. Yu, G. Li, and L. Yang, "A tunable ultrabroadband ultrathin terahertz absorber using graphene stacks," *IEEE Antennas Wireless Propag. Lett.*, vol. 16, pp. 1115–1118, 2017.
[9] A. Arsanjani, M. Biabanifard, and M. S. Abrishamian, "A novel analytical method for designing a multi-band, polarization-insensitive and wide angle graphene-based THz absorber," *Superlattices Microstruct.*, vol. 128, pp. 157–169, Apr. 2019.
[10] L. Ye, X. Chen, G. Cai, J. Zhu, N. Liu, and Q. Liu, "Electrically tunable broadband terahertz absorption with hybrid-patterned graphene metasurfaces," *Nanomaterials*, vol. 8, no. 8, pp. 562–572, 2018.
[11] L. Ye, F. Zeng, Y. Zhang, X. Xu, X. Yang, and Q. H. Liu, "Frequency-reconfigurable wide-angle terahertz absorbers using single- and double-layer decussate graphene ribbon arrays," *Nanomaterials*, vol. 8, no. 10, p. 834, 2018.
[12] G. Yao, F. Ling, J. Yue, C. Luo, J. Ji, and J. Yao, "Dual-band tunable perfect metamaterial absorber in the THz range," *Opt. Express*, vol. 24, no. 2, pp. 1518–1527, 2016.
[13] S. Biabanifard, M. Biabanifard, S. Asgari, S. Asadi, and M. C. E. Yagoub, "Tunable ultra-wideband terahertz absorber based on graphene disks and ribbons," *Opt. Commun.*, vol. 427, pp. 418–425, Nov. 2018.
[14] M. Biabanifard and M. S. Abrishamian, "Ultra-wideband terahertz graphene absorber using circuit model," *Appl. Phys. A, Solids Surf.*, vol. 124, no. 12, p. 826, Dec. 2018.
[15] L. Ye, F. Zeng, Y. Zhang, and Q. H. Liu, "Composite graphene-metal microstructures for enhanced multiband absorption covering the entire terahertz range," *Carbon*, vol. 148, pp. 317–325, Jul. 2019.
[16] L. Ye, Y. Chen, G. Cai, N. Liu, J. Zhu, Z. Song, and Q. H. Liu, "Broadband absorber with periodically sinusoidally-patterned graphene layer in terahertz range," *Opt. Express*, vol. 25, no. 10, p. 11223, May 2017.
[17] M. S. Islam, J. Sultana, M. Biabanifard, Z. Vafapour, M. J. Nine, A. Dinovitser, C. M. B. Cordeiro, B. W.-H. Ng, and D. Abbott, "Tunable localized surface plasmon graphene metasurface for multiband superabsorption and terahertz sensing," *Carbon*, vol. 158, pp. 559–567, Mar. 2020.
[18] A. Andryieuski and A. V. Lavrinenko, "Graphene metamaterials based tunable terahertz absorber: Effective surface conductivity approach," *Opt. Express*, vol. 21, no. 7, p. 9144, Apr. 2013.

[19] M. Biabanifard and M. S. Abrishamian, "Multi-band circuit model of tunable THz absorber based on graphene sheet and ribbons," *AEU-Int. J. Electron. Commun.*, vol. 95, pp. 256–263, Oct. 2018.
[20] A. Alù, M. G. Silveirinha, and N. Engheta, "Transmission-line analysis of ε-near-zero–filled narrow channels," *Phys. Rev. E, Stat. Phys. Plasmas Fluids Relat. Interdiscip. Top.*, vol. 78, no. 1, 2008, Art. no. 016604.
[21] N. Engheta, "Circuits with light at nanoscales: Optical nanocircuits inspired by metamaterials," *Science*, vol. 317, no. 5845, pp. 1698–1702, Sep. 2007.
[22] N. Engheta, A. Salandrino, and A. Alù, "Circuit elements at optical frequencies: Nanoinductors, nanocapacitors, and nanoresistors," *Phys. Rev. Lett.*, vol. 95, no. 9, Aug. 2005, Art. no. 095504.
[23] Y. Li, I. Liberal, C. D. Giovampaola, and N. Engheta, "Waveguide metatronics: Lumped circuitry based on structural dispersion," *Sci. Adv.*, vol. 2, no. 6, Jun. 2016, Art. no. e1501790.
[24] M. Biabanifard and M. S. Abrishamian, "Circuit modeling of tunable terahertz graphene absorber," *Optik*, vol. 158, pp. 842–849, Apr. 2018.
[25] A. Khavasi, "Design of ultra-broadband graphene absorber using circuit theory," *J. Opt. Soc. Amer. B, Opt. Phys.*, vol. 32, no. 9, pp. 1941–1946, Sep. 2015.
[26] H. J. Yoon, D. H. Jun, J. H. Yang, Z. Zhou, S. S. Yang, and M. M.-C. Cheng, "Carbon dioxide gas sensor using a graphene sheet," *Sens. Actuators B, Chem.*, vol. 157, no. 1, pp. 310–313, Sep. 2011.
[27] X. Liang, Z. Fu, and S. Y. Chou, "Graphene transistors fabricated via transfer-printing in device active-areas on large wafer," *Nano Lett.*, vol. 7, no. 12, pp. 3840–3844, Dec. 2007.
[28] J. Balakrishnan, B. M. Fischer, and D. Abbott, "Sensing the hygroscopicity of polymer and copolymer materials using terahertz time-domain spectroscopy," *Appl. Opt.*, vol. 48, no. 12, p. 2262, Apr. 2009.
[29] *Topas Advanced Polymers*. [Online]. Available: https://topas.com/topas-advanced-polymers-inc
[30] P. D. Cunningham, N. N. Valdes, F. A. Vallejo, L. M. Hayden, B. Polishak, X.-H. Zhou, J. Luo, A. K.-Y. Jen, J. C. Williams, and R. J. Twieg, "Broadband terahertz characterization of the refractive index and absorption of some important polymeric and organic electro-optic materials," *J. Appl. Phys.*, vol. 109, no. 4, Feb. 2011, Art. no. 043505.
[31] L. Ju, B. Geng, J. Horng, C. Girit, M. Martin, Z. Hao, H. A. Bechtel, X. Liang, A. Zettl, and Y. R. Shen, "Graphene plasmonics for tunable terahertz metamaterials," *Nature Nanotechnol.*, vol. 6, no. 10, p. 630, 2011.
[32] A. Vakil and N. Engheta, "Transformation optics using graphene," *Science*, vol. 332, no. 6035, pp. 1291–1294, Jun. 2011.
[33] A. Khavasi and B. Rejaei, "Analytical modeling of graphene ribbons as optical circuit elements," *IEEE J. Quantum Electron.*, vol. 50, no. 6, pp. 397–403, Jun. 2014.
[34] D. K. Cheng, *Field and Wave Electromagnetics*. London, U.K.: Pearson, 1989.
[35] G. W. Hanson, "Dyadic Green's functions and guided surface waves for a surface conductivity model of graphene," *J. Appl. Phys.*, vol. 103, no. 6, Mar. 2008, Art. no. 064302.
[36] S. A. Mikhailov, "Non-linear electromagnetic response of graphene," *Europhys. Lett.*, vol. 79, no. 2, p. 27002, Jul. 2007.
[37] G. W. Hanson, "Quasi-transverse electromagnetic modes supported by a graphene parallel-plate waveguide," *J. Appl. Phys.*, vol. 104, no. 8, Oct. 2008, Art. no. 084314.
[38] S. E. Hosseininejad, N. Komjani, and M. T. Noghani, "A comparison of graphene and noble metals as conductors for plasmonic one-dimensional waveguides," *IEEE Trans. Nanotechnol.*, vol. 14, no. 5, pp. 829–836, Sep. 2015.
[39] M. Trushin and J. Schliemann, "Anisotropic photoconductivity in graphene," *Europhys. Lett.*, vol. 96, no. 3, p. 37006, Nov. 2011.
[40] P. A. George, J. Strait, J. Dawlaty, S. Shivaraman, M. Chandrashekhar, F. Rana, and M. G. Spencer, "Ultrafast optical-pump terahertz-probe spectroscopy of the carrier relaxation and recombination dynamics in epitaxial graphene," *Nano Lett.*, vol. 8, no. 12, pp. 4248–4251, Dec. 2008.
[41] J. Hu, X. Ruan, and Y. P. Chen, "Thermal conductivity and thermal rectification in graphene nanoribbons: A molecular dynamics study," *Nano Lett.*, vol. 9, no. 7, pp. 2730–2735, Jul. 2009.
[42] V. Ryzhii, M. Ryzhii, and T. Otsuji, "Negative dynamic conductivity of graphene with optical pumping," *J. Appl. Phys.*, vol. 101, no. 8, Apr. 2007, Art. no. 083114.
[43] F. Tabatabaei, M. Biabanifard, and M. S. Abrishamian, "Terahertz polarization-insensitive and all-optical tunable filter using kerr effect in graphene disks arrays," *Optik*, vol. 180, pp. 526–535, Feb. 2019.
[44] C. R. Dean, A. F. Young, I. Meric, C. Lee, L. Wang, S. Sorgenfrei, K. Watanabe, T. Taniguchi, P. Kim, K. L. Shepard, and J. Hone, "Boron nitride substrates for high-quality graphene electronics," *Nature Nanotechnol.*, vol. 5, no. 10, pp. 722–726, Oct. 2010.
[45] A. Avsar, T.-Y. Yang, S. Bae, J. Balakrishnan, F. Volmer, M. Jaiswal, Z. Yi, S. R. Ali, G. Güntherodt, B. H. Hong, and B. Beschoten, "Toward wafer scale fabrication of graphene based spin valve devices," *Nano Lett.*, vol. 11, no. 6, pp. 2363–2368, Jun. 2011.
[46] L. Banszerus, M. Schmitz, S. Engels, J. Dauber, M. Oellers, F. Haupt, K. Watanabe, T. Taniguchi, B. Beschoten, and C. Stampfer, "Ultrahigh-mobility graphene devices from chemical vapor deposition on reusable copper," *Sci. Adv.*, vol. 1, no. 6, Jul. 2015, Art. no. e1500222.
[47] R. Xing and S. Jian, "A dual-band THz absorber based on graphene sheet and ribbons," *Opt. Laser Technol.*, vol. 100, pp. 129–132, Mar. 2018.
[48] C. Gong, M. Zhan, J. Yang, Z. Wang, H. Liu, Y. Zhao, and W. Liu, "Broadband terahertz metamaterial absorber based on sectional asymmetric structures," *Sci. Rep.*, vol. 6, no. 1, Oct. 2016, Art. no. 32466.
[49] Y. Wen, W. Ma, J. Bailey, G. Matmon, and X. Yu, "Broadband terahertz metamaterial absorber based on asymmetric resonators with perfect absorption," *IEEE Trans. THz Sci. Technol.*, vol. 5, no. 3, pp. 406–411, May 2015.
[50] B.-X. Wang, L.-L. Wang, G.-Z. Wang, W.-Q. Huang, X.-F. Li, and X. Zhai, "Theoretical investigation of broadband and wide-angle terahertz metamaterial absorber," *IEEE Photon. Technol. Lett.*, vol. 26, no. 2, pp. 111–114, Jan. 15, 2014.
[51] J.-M. Jin, *The Finite Element Method in Electromagnetics*. Hoboken, NJ, USA: Wiley, 2015.
[52] Z. Wang, J. Lee, K. He, J. Shan, and P. X.-L. Feng, "Embracing structural nonidealities and asymmetries in two-dimensional nanomechanical resonators," *Sci. Rep.*, vol. 4, no. 1, pp. 3919–3925, May 2015.
[53] M. Abbasi, M. Biabanifard, and M. S. Abrishamian, "Design of symmetrical wide-angle graphene-based mid-infrared broadband perfect absorber based on circuit model," *Photon. Nanostruct.-Fundam. Appl.*, vol. 36, Sep. 2019, Art. no. 100729.

MOHAMMAD BIABANIFARD was born in Tehran, Iran, in 1992. He received the B.S. degree in telecommunication engineering, in 2015. He is currently pursuing the M.Sc. degree in telecommunications with the Department of Electrical Engineering, K. N. Toosi University of Technology (KNTU). He is also a Senior Researcher with the Iran Analog Research Group and has numerous scientific collaborations with a number of research teams and technological laboratories. His current research interests are in the areas of plasmonics, terahertz metamaterials, nanophotonics, and numerical modeling of electromagnetics. His previous research interests include image processing, coding, robotics, and integrated circuits.

ARASH ARSANJANI was born in Kerman, Iran, in 1992. He received the B.Sc. degree in electrical engineering from the Shahid Bahonar University of Kerman, Kerman, Iran in 2015, and the M.Sc. degree in electrical engineering from the K. N. Toosi University of Technology, Tehran, Iran, in 2018. He is currently pursuing the Ph.D. degree with the Graz University of Technology, Graz, Austria. His research interests include graphene technology, terahertz applications, microwave and RF components, microwave filters, and microwave antennas. His current field of study includes low-loss microwave components for satellite applications.

MOHAMMAD SADEGH ABRISHAMIAN (Member, IEEE) received the B.S. degree from the High Institute of Telecommunication, Tehran, Iran, in 1970, the M.S. degree from Northrop University, Inglewood, CA, USA, in 1978, and the Ph.D. degree from Bradford University, Bradford, U.K., in 1996, all in electrical engineering. For the past 30 years, he has been a Faculty Member with the K. N. Toosi University of Technology, Tehran, Iran, where he is currently a Professor. His research interests are penetration and scattering of electromagnetic (EM) waves, photonic crystals, plasmonics, and computational electromagnetics.

DEREK ABBOTT (Fellow, IEEE) was born in London, U.K., in 1960. He received the B.Sc. degree (Hons.) in physics from Loughborough University, U.K., in 1982, and the Ph.D. degree in electrical and electronic engineering from The University of Adelaide, Adelaide, Australia, in 1995, under the supervision of K. Eshraghian and B. R. Davis. From 1978 to 1986, he was a Research Engineer with the GEC Hirst Research Centre, London. From 1986 to 1987, he was a VLSI Design Engineer with Austek Microsystems, Australia. Since 1987, he has been with The University of Adelaide, where he is currently a Full Professor with the School of Electrical and Electronic Engineering. He has coedited the book *Quantum Aspects of Life* (Imperial College Press), and coauthored the books *Stochastic Resonance* (Cambridge University Press) and *Terahertz Imaging for Biomedical Applications* (Springer-Verlag). His interests are in the areas of multidisciplinary physics and electronic engineering applied to complex systems. His research programs span a number of areas of stochastics, game theory, photonics, biomedical engineering, and computational neuroscience. He is a Fellow of the Institute of Physics (IOP). He received the number of awards, including the South Australian Tall Poppy Award for Science, in 2004, the Premier's SA Great Award in Science and Technology for outstanding contributions to South Australia, in 2004, the Australian Research Council (ARC) Future Fellowship, in 2012, the David Dewhurst Medal, 2015, the Barry Inglis Medal, in 2018, and the M. A. Sargnet Medal for eminence in engineering, in 2019. He has served as an editor and/or a guest editor for a number of journals, including the IEEE JOURNAL OF SOLID-STATE CIRCUITS, *Journal of Optics B* (IOP), *Microelectronics Journal* (Elsevier), Proceedings of the IEEE, and the IEEE PHOTONIC JOURNAL. He is currently on the Editorial Boards of IEEE ACCESS, *Scientific Reports* (Nature), and *Royal Society Open Science*.